DESERT BASED ABSOLUTE CALIBRATION OF VISIBLE SENSORS

Rajendra Bhatt [a], David R. Doelling [b], Benjamin R. Scarino [a], Daniel L. Morstad [a]

[a] Science Systems and Applications, Inc., Hampton, VA 23666
[b] NASA Langley Research Center, Hampton, VA 23666

ABSTRACT

Post-launch calibration and characterization of Geostationary Earth Observing (GEO) satellite sensors, which lack on-board visible calibration, is a keenly felt need in many applications for studying long-term global climate changes. This paper proposes a vicarious technique of calibrating GEO visible sensors for the Clouds and the Earth's Radiant Energy System (CERES) project, using a kernel-based bidirectional reflectance distribution function (BRDF) model derived over an invariant desert site. The technique is illustrated with two Meteosat-9 visible channels, 0.65um and 0.86um, whose radiometric gains have been computed using a BRDF model of Libya-4 desert site. The Libya-4 BRDF model is TOA based and is derived from ten years of clear-sky Aqua observations over this site. The calibration results are validated by a direct comparison with the corresponding gains derived from the GEO-to-MODIS ray-matching technique.

Index Terms— Invariant sites, Libya-4, CERES, Meteosat, BRDF

1. INTRODUCTION

The primary approach of calibrating GEO visible sensors for the CERES project has been based on ray matching using a reference sensor, which involves inter-comparison of co-incident, co-angled, and co-located regions scanned by both GEO and MODIS sensors over an equatorial domain under the GEO sub-satellite point [1]. Although this technique provides robust calibration of GEO sensors, it is limited in applicability to only those GEOs active during the MODIS timeframe. This paper describes an alternative desert-based calibration approach that not only validates the GEO-to-MODIS ray-matching technique, but also demonstrates a potential to be applicable to historical GEO sensors. The use of invariant desert sites for relative trending of the radiometric gain of a satellite sensor has been well accepted. However, use of invariant deserts as an independent absolute calibration target is still being developed. This paper illustrates an approach of using a bidirectional reflectance model over a Libyan Desert site, based on Aqua-MODIS as the absolute calibration reference. The model is then used to predict the TOA reflectance for a GEO visible sensor under given viewing and solar angular conditions, and derive the radiometric gain for the sensor.

2. METHODOLOGY

2.1. Characterization of Libya-4

Most desert-based calibration approaches characterize the desert surface and then model the atmosphere to predict the reference TOA radiance to calibrate a sensor. This approach characterizes the desert at the TOA, which assumes the atmosphere above the desert is predictable. To illustrate, the Libya-4 desert site (28.55°N latitude and 23.39°E longitude) is observed by the GEO Meteosat-9 satellite continuously at the same view zenith angle of 42.1°. Meteosat-9 has a fixed imaging schedule and thus provides annually repeating time-consistent data each day, which is useful for analyzing the seasonal variation in the instrument's response to an invariant terrestrial target. Since the desert is usually clear, a simple standard deviation threshold of the pixel level counts contained within the Libya-4 domain is applied to determine the clear-sky observations. Figure 1 shows over four years of clear-sky observations of the Libya-4 site from the Meteosat-9 visible sensor (0.65μm) acquired at 10:30 GMT, which is close to the local noontime. The Meteosat-9 visible pixel (3-km nominal) raw counts were averaged after subtracting the known space count value of 51. The mean raw count is then converted to absolute TOA radiance using the radiometric gains of Meteosat-9 derived through ray-matching inter-calibration with Aqua-MODIS [1]. The consistent repeating cycle of the TOA radiance every year suggests that the combined surface and clear-sky atmosphere column were invariant over multiple years. The average inter-annual variability in the observed Meteosat-9 TOA radiance made on a certain day at near local noontime is found to be less than 0.8%.

2.2. TOA BRDF model of Libya-4

Ten years of calibrated and clear-sky MODIS observations over Libya-4, which include all view and solar zenith angles, have been used to derive a kernel-driven TOA BRDF model for this site [2][3][4]. Aqua-MODIS is chosen, since it the better characterized and more stable of the MODIS sensors [5]. The BRDF equation is expressed as:

$$\rho(\theta_s, \theta_v, \phi) = k_0 + k_1 F_1(\theta_s, \theta_v, \phi) + k_2 F_2(\theta_s, \theta_v, \phi),$$

where the $\rho(\theta_s, \theta_v, \phi)$ is the predicted bidirectional reflectance in a particular direction and is a function of solar zenith (θ_s), view zenith (θ_v), and relative azimuth (ϕ) angles. Functions F1 and F2 are derived explicitly for each combination of solar and viewing angular conditions using the geometric and volume scattering components as described by Roujean et al. [2], and k0, k1, and k2 are surface specific parameters that are derived empirically using ten years of calibrated Aqua TOA reflectance over Libya-4 [3]. Once the model parameters are computed, the TOA reflectance for any similar sensor imaging Libya-4 can be predicted from the model using the given solar and viewing angular conditions.

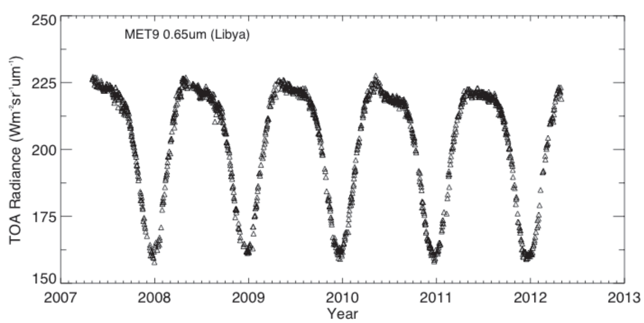

Fig. 1. Calibrated Meteosat-9 TOA radiance derived over Libya 4 using clear-sky data acquired at 10:30 GMT.

To determine how accurately the Aqua-MODIS based model reproduces angular reflectances, that Meteosat-9 is expected to observe over Libya-4 at 11:30 GMT time, which is coincident with the Aqua overpass time, the model is first tested with Aqua itself for the observations restricted to view zenith angles between 40° and 50° and relative azimuth angles in the backscatter direction (90° to 180°). Figure 2 shows the timeline of the observed and predicted TOA reflectances. The red circles indicate the predicted reflectances from the model that was derived using all Aqua-MODIS observations with a view angle less than 50°. It clearly shows that the model does not retain the reflectance structure of the Meteosat-9 predicted angles. The model was recomputed only using Aqua-MODIS measurements within 40°<VZA<50° and 90°<RZA<180°. The predicted reflectances from this model are shown by green circles in Figure 2 and are within 1.07% of the observations.

2.3. Spectral band differences

In case the spectral response function (SRF) of the GEO visible sensor is different than that of MODIS, a spectral band adjustment factor (SBAF) must be applied to account for those differences. Figure 3 shows the SRFs of Aqua (0.65µm and 0.86µm) and Meteosat-9 (0.65µm and 0.80µm) visible channels.

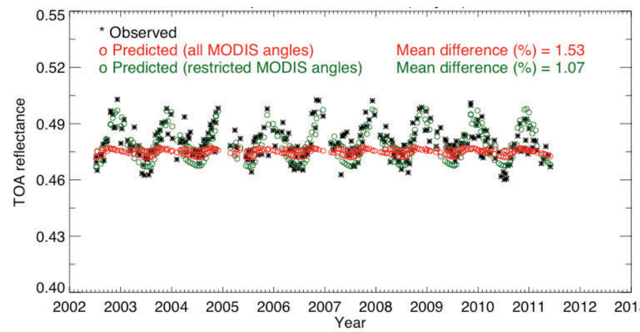

Fig. 2. Observed Aqua-MODIS reflectances, restricted within the angular domain of (40°<VZA<50°) and (90°<RZA<180°), and the associated modeled Aqua reflectance, derived from observations using the same angular domain (green circles) and all observations less than 50° view angle (red circles) over Libya-4.

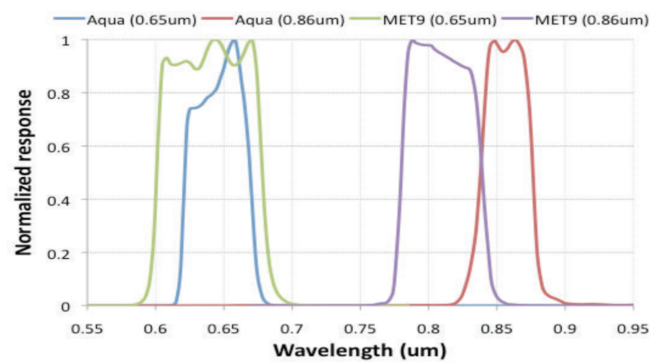

Fig. 3. SRFs of MODIS and Meteosat-9 visible channels.

In this study, the high-resolution reflected solar spectra measured by SCIAMACHY over the Libya-4 site is used to derive the SBAF between the Meteosat-9 and MODIS visible channels, using the technique described by Doelling et al. [6] The SCIAMACHY spectra of Libya 4 are first convolved with the SRFs of Meteosat-9 and MODIS visible channels to estimate the pseudo-imager radiances for both sensors. The Meteosat-9 pseudo-radiances are then regressed against the Aqua pseudo-radiances, and the forced slope (regression through zero) is used as the SBAF.

The SBAF regressions for the MODIS and Meteosat-9 channels are shown in Figure 4. The Meteosat-9 0.65µm channel exhibits a consistent SBAF for all seasons. However, the SBAF regression for the 0.80µm channel indicates an apparent seasonal cycle, which means a singe SBAF might not be good enough to account for the spectral differences between these two channels. Therefore, the

SBAF regression for the Meteosat-9 0.80µm and Aqua 0.86µm channels is broken down to seasons and applied accordingly.

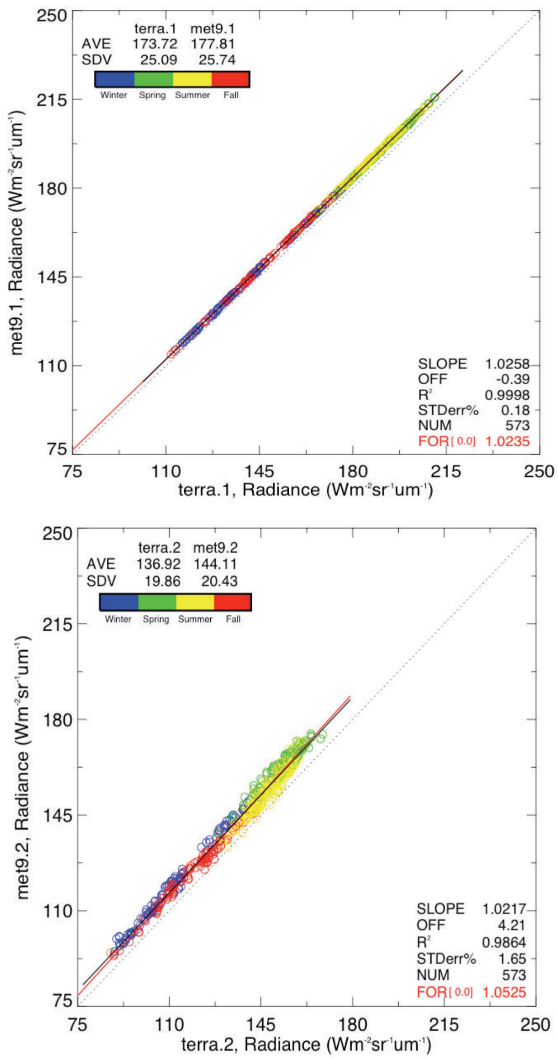

Fig. 4. The regression of SCIAMACHY pseudo radiances for the Meteosat-9 0.65µm and Aqua 0.65µm channels (top), and the Meteosat-9 0.80µm and Aqua 0.86µm channels (bottom). The radiances are color coded according to season.

SBAF correction when performed in radiance normalizes both the incoming solar and atmospheric absorption between the two spectral bands. To determine the portion accounting for the out of band atmospheric absorption, The solar component can be removed by computing the Met-9/Aqua ratio between the two channel TOA solar radiances and comparing them to the regression in figure 5. The TOA solar radiance for Meteosat-9 and Aqua-MODIS 0.65µm band is 516.3 and 509.8 Wm-2sr-1µm-1, respectively. This equates to 1.0128 and when compared with 1.0235 from figure 5 indicates that half of the difference is from the incoming solar and the other half from out of band absorption. Similarly, the incoming solar is 354.6 and 316.7 for Met-9 and Aqua, respectively, for the 0.86µm band and the incoming solar ratio is 1.1195. Although Meteosat-9 has a greater incoming solar radiance, atmospheric absorption in the Met-9 band is much greater than in the Aqua 0.86µm band and reduces the SBAF correction to 1.0525. If only the channel solar incoming was accounted for, the Met-9 0.65µm band would be underestimated by ~1% and the 0.86µm band overestimated by ~7%.

The SBAF is applied to the output of the Aqua-based BRDF model in order to arrive at a correct predicted TOA radiance for Meteosat-9. At last, the gains of the Meteosat-9 visible channels are computed from the SBAF corrected TOA radiances estimated from the BRDF model by using the following equation:

$$\text{TOA radiance} = \text{Gain} \times (\text{Raw count} - \text{Space count})$$

The so derived gains are averaged on a monthly-basis and are compared with those obtained from GEO-to-MODIS ray-matched technique.

3. RESULTS

The Aqua 0.65µm based TOA BRDF model of Libya-4 was applied to the Meteosat-9 0.65µm mean visible raw-count acquired over the same region from the 11:30 GMT images to derive its radiometric gain. Figure 5 displays the monthly mean desert and ray-matched gains of the Meteosat-9 0.65µm channel during 2007-2012, with linear regressions applied to both techniques. A direct comparison of their lifetime mean gains shows consistency within 0.2%, while the standard error of the desert method is slightly higher than that of the ray-matched calibration. These results show the effectiveness of transferring calibration via a kernel-based TOA BRDF model, validating that the desert is stable and characterizable from the TOA.

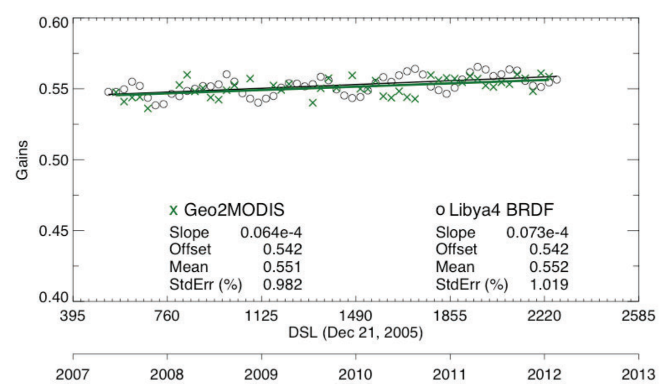

Fig. 5. Comparison of Meteosat-9 visible channel (0.65 µm) monthly radiometric gains derived from Aqua-MODIS/Meteosat-8 ray matching (red Xs) and the Libya-4 BRDF approach (black circles).

Similarly, the Meteosat-9 0.80μm channel is calibrated using the TOA BRDF model of Libya-4 based on the Aqua 0.86μm observations. Figure 6 compares the Meteosat-9 0.86μm channel monthly gains derived from Aqua-MODIS ray-matching and Libya-4 BRDF approach. The uncertainty of the ray-matching and desert methods is less than 2%. The desert-based gains exhibit some residual seasonal cycle, presumably caused by the seasonal dependence of the absorption effects in the Meteosat-9 0.80μm channel. The means of the two sets of gains agree within 1.7%, which is within the uncertainty level of both techniques. This difference may be attributed to the uncertainty in the seasonal SBAFs that were calculated using SCIAMACHY data limited to ~15° VZA and were applied to Aqua observations with VZA between 40°and 50°.

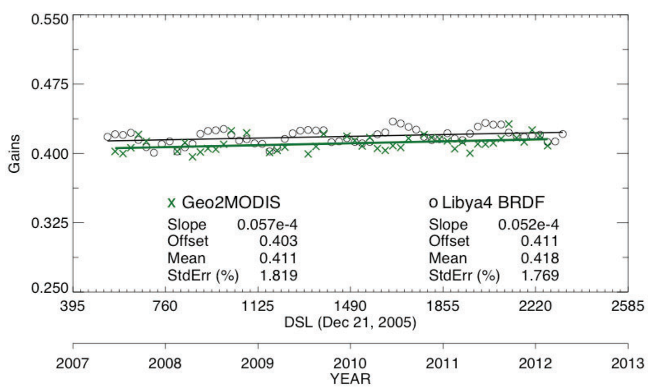

Fig. 6. Comparison of Meteosat-9 visible channel (0.80 μm) monthly radiometric gains derived from Aqua-MODIS/Meteosat-8 ray matching (red Xs) and the Libya-4 BRDF approach (black circles).

4. CONCLUDING REMARKS

Invariant desert sites have been used as an independent reference for assessing the post-launch radiometric stability of visible sensors. A methodology has been developed to characterize these Earth targets from the TOA. It is dependent on the combined stability of the ground site and the atmospheric column above it. Libya-4 was used as the test site in this study. Four years of consistent time daily clear-sky TOA observations from the Meteosat-9 satellite showed an average daily inter-annual variability of less than 0.8% for Libya-4. A kernel-based TOA BRDF model was developed using ten years of calibrated Aqua radiances. When tested with the Aqua data itself, the predicted TOA reflectance agreed with the observed TOA reflectance within 1.07% for Aqua 0.65μm channel, indicating the model is robust. The Aqua-based BRDF model of Libya-4 was then used to transfer calibration to Meteosat-9 visible channels, and the results were compared with those obtained from GEO-to-MODIS ray-matching technique. The results were consistent within 0.2% and 1.7%, respectively, for bands 0.65μm and 0.80μm channels of Meteosat-9. In order to account for the spectral band differences between Meteosat-9 and MODIS channels, SBAF were derived using the Libya-4 reflected solar spectra obtained from SCIAMACHY hyper-spectral observations. This method will be further incorporated with other geostationary as well as polar orbiting satellites.

5. ACKNOWLEDGEMENTS

The NASA science mission directory through the CERES project at the NASA-Langley research center funded this research.

6. REFERENCES

[1] P.L. Minnis, L. Nguyen, D.R. Doelling, D.F. Young, and W.F. Miller, “Rapid calibration of operational and research meteorological satellite images, Part I: Evaluation of Research Satellite Visible Channels as References,” *Journal of Atmospheric and Oceanic Technology Vol. 19,* 1233-1249, 2002.

[2] J.L. Roujean, M.J.Leroy, and P.Y.Deschamps, “A bidirectional reflectance model of the earth’s surface for the correction of remote sensing data,” *Journal of Geophysical Research*, 20455–20468, 1992.

[3] A. Angal, X. Xiong, T. Choi, G. Chander, and A. Wu, “Using the Sonoran and Libyan Desert test sites to monitor the temporal stability of reflective solar bands for Landsat 7 enhanced thematic mapper plus and Terra moderate resolution imaging spectroradiometer sensors,” *Journal of Applied Remote Sensing*, Vol. 4, 043524, 14 April 2010.

[4] D.L. Morstad, D.R. Doelling, R. Bhatt, and B. Scarino, The CERES calibration strategy of the geostationary visible channels for CERES cloud and flux products, *Proc. SPIE 8153*, 815316 (2011); doi:10.1117/12.894650.

[5] A. Wu, X. Xiong, D. R. Doelling, D. L. Morstad, A. Angal, and R. Bhatt, “Characterization of Terra and Aqua MODIS VIS, NIR, and SWIR spectral band calibration stability,” *IEEE Transactions on Geoscience and Remote Sensing,* submitted Nov. 28, 2011.

[6] D.R. Doelling, C. Lukashin, P. Minnis, B. Scarino, and D. Morstad, "Spectral Reflectance Corrections for Satellite Intercalibrations Using SCIAMACHY Data," *Geoscience and Remote Sensing Letters, IEEE*, vol.9, no.1, pp.119-123, Jan. 2012 doi: 10.1109/LGRS.2011.2161751.